Thermoelectric properties of carbonaceous solids

Francesco Miccio♠

Istituto di Scienza e Tecnologia dei Materiali Ceramici, CNR-ISTEC Faenza, Via Granarolo, 64 - 48018 Faenza (RA), Italy

http://carbonlett.org

The application of thermoelectric measurements to characterize carbonaceous materials, such as graphite and chars, can be helpful for monitoring the chemical/physical evolution of the material during gasification, which occurs upon steps of gas diffusion and heterogeneous chemical reactions at moderate and high temperature. The present article reports on an experimental study on the application of thermoelectric measurements for qualitative and semi-quantitative characterization of carbonaceous materials, such as graphite and chars, also in course of high temperature chemical conversion.

Among carbonaceous fuels, graphite and cokes are poorly reactive, whereas the reactivity increases moving from coal to biomass derived chars (e.g., carbonized wood) [1]. To date, investigations have normally been carried out in thermo-balance, providing information on the weight loss of the sample during the test interval as well as on the evolution of gaseous products, when coupled with mass-spectrometry. In addition to the morphology and the degree of order at molecular level being relevant in determining the gasification reactivity of carbons, the presence of some elements in the ashes (e.g., alkalis) can accelerate the carbon conversion [2]. Conversely, high ash content has a negative impact because of the increased diffusional resistances and heat dispersion [3]. The enlargement of the porosity and the possible melting and coalescence of ash inclusions [4] are also correlated to some degree to the loss of reactivity. During carbon gasification tests in a thermo-gravimetric (TG) apparatus, the weight loss enables quantitative characterization of the fuel reactivity, but the internal structural evolution of the particles cannot be detected. Notably, it is difficult to perform on line measurements in the core of the oxidizing particle (for example, X-ray tomography to obtain a 3-D map of pores and materials) during conversion [5].

The thermoelectric or Seebeck effect is the generation of an electromotive force (EMF) in a solid, when a gradient of temperature is established for any reason [6]. The thermoelectric effect is induced by the interactions between heat carriers in the solid and thermally excited electrons, leading to the accumulation of electrons and holes at the opposite sides of the body [7]. The ratio between the EMF, measured in µV, and the temperature difference is defined as the Seebeck coefficient [8], which in most cases is referred to as a temperature gap of 100 K. The Seebeck coefficient is an absolute property of a material; however, for practical reasons, it is usually referred to the property of a standard element, in most cases Pt. Technological applications of the Seebeck effect can be found in temperature measurements by thermocouples, in sensors for measuring gas concentration, and in micro-generation of electricity.

The generated EMF depends on the temperature difference between the body ends as well as on the properties of the material. The thermoelectric effect of a pure material is the combination of various phenomena including the electrical conduction via electrons and holes, the thermal conduction by electrons and phonons, and the interactions between heat and electrical carriers in a solid [9]. Furthermore, in practical materials the presence of defects, cracks, and dopants may significantly alter the thermoelectric characteristics [7]. In general, metals have appreciable thermoelectric properties thanks to their high electrical conductivity, whereas electrical insulators generally exhibit a very small Seebeck effect. Composite or doped solid state materials, such as semi-conductors, show large thermoelectric effects, some orders of magnitude higher than metals, because they can be designed to have high electrical conductivity with low lattice thermal conductivity [10]. Currently, there

Table 1. Properties of the parent fuels and major elements detected in the ashes (% by mass)

Parent fuels	Type	Size (mm)	Bulk density (kg m^{-3})	Porosity (%, by Hg intrusion)	Median pore size (μm)	Fixed C (%, dry)	Ash/ fixed C ratio (%)	Al	Ba	Fe	K	Mg	Si
Graphite	Rod	4.85 diameter	1621	14.61	0.69	99.0	1.0	<0.01	0	0.123	0	0	0
Sulcis coal	Bar	approx. 5 × 10	1167[*]	23.91[*]	26.9	43.4	34.0	0.18	0.04	0.77	0.01	0.13	0.15
Beech wood	Rod	10.0 diameter	501[*]	60.74[*]	15.8	16.5	3.0	0	0	0	0.02	<0.01	<0.01

[*]Values for char.

is strong interest in developing novel thermoelectric materials, in particular for smart power generation. Thus, the capacity to fabricate nanodispersed composites greatly favours the achievement of very high performance in heat to electricity conversion via the Seebeck effect [11]. The characteristics of several materials were recently reviewed by Gaultois et al. [12], providing a comparative overview based on more than 18,000 data-points obtained from the literature, including elements and oxides as well as the high-performing half-Heusler compounds [13]. The Seebeck coefficient also increases with temperature [14] because of the larger availability of thermally excited electrons in the conduction band. For instance, the absolute Seebeck coefficient rises by factors of 2.2 and 3.1, moving from 273 to 673 K for Cu and Pt, respectively [15].

Investigations on the application of thermoelectric measurements for detecting modifications in microstructure of metal alloys were carried out by Acosta and Sevini [16]. They reported that structural changes of the material due to nuclear irradiation can be revealed by simple thermoelectric tests. Since graphite and carbons are conductors of electricity, they also have thermoelectric properties, which were investigated for micro-generation by Luo et al. [17]. The Seebeck coefficient of carbon referenced to Pt is positive and equal to +220 μV for a temperature difference of 100 K, having the same order of magnitude of that of metals such as Cu, Au, Al, and Pb [14]. Therefore, this property opens the possibility to apply thermoelectric measurements for characterizing carbonaceous samples that are either unconverted or partially gasified and for revealing modifications of the composition/structure.

An experimental apparatus having two horizontal copper electrodes located at variable distance in order to sustain the carbonaceous sample (rod or bar with a length of about 50 mm) was assembled to carry out the thermoelectric measurements. A glass bar is located over the center of the specimen in order to ensure good contact with the electrodes. The first electrode can be heated by means of electrical resistance up to 240°C, whereas the second is kept at room temperature. Two type K thermocouples are inserted in the electrodes for measuring the temperature in each element and the temperature difference ΔT $= T_h - T_c$ between hot and cold electrodes. Copper wires departing from the electrodes are connected to the input terminals of a digital nano-voltmeter (model: Keithley 2182A), with care to avoid any junction of different conductors that would induce additional Seebeck effects. Since the voltmeter is inserted between cold and hot copper electrodes with a positive end at the hot

side, it measures the opposite EMF of the pair sample/Cu [9]. The measured EMF, on the order of dozens of microvolts, is acquired along with the signals from the thermocouples by a computer for further elaboration.

A platinum lamina with purity 999/1000 has been used as a reference material to check the reliability of the thermoelectric apparatus. Although the experimental rig was not extremely sophisticated in order to perform steady measurements under a controlled atmosphere [18], the resulting experimental error was acceptable for a practical scope.

Carbonaceous materials used during the tests were graphite and chars obtained by treating coal and wood at 800°C in a muffle furnace under an argon atmosphere. Table 1 reports the properties of the three tested materials in terms of geometric dimensions, bulk density, porosity, average pore size, fixed carbon content, and the ratio between ash and fixed C in the parent fuels. Large differences exist among the samples, in particular in relation to the internal structure, with the chars exhibiting higher porosity and higher median pore size than the graphite.

The X-ray diffraction analysis of the graphite, performed with a Bruker D8 Advance instrument (Karlsruhe, Germany), revealed that the basal layers of the material are disposed along the longitudinal direction of the rods and that the main element in the ash is iron. It is well known that the mechanical and electrical properties of graphite largely depend on the orientation with respect to the basal plane [19]. Sulcis coal is a reactive lignite with high content of volatiles and sulphur [20]. Beech wood is a typical biomass fuel, having low ash content. The analysis of the ash was carried out upon dissolution of the fuel in HNO_3/ H_2O_2 and via an inductively coupled plasma mass spectrometer (ICP-MS) analysis. The major elements detected in the fuels are reported in Table 1. It is worth noting that Fe was revealed to a large extent in both graphite and Sulcis coal.

The reactivity toward gasification of the carbonaceous samples has been determined by a preliminary analysis carried out in a thermogravimetric apparatus (STA 449 Jupiter Netzsch; Geratebau, Selb, Germany) at 900°C in an atmosphere of Ar 50% - CO_2 50% vol. Graphite exhibits very low reactivity, only 20% conversion achieved after 420 min. Sulcis coal char has an intermediate reactivity between the graphite and the highly reactive beech wood char.

A Raman spectroscopy analysis of graphite, beech wood char, and Sulcis coal char was carried out with a Horiba XploRA Raman microscope system following the procedure reported by Minutolo et al. [21]. The Raman spectra were recorded in a
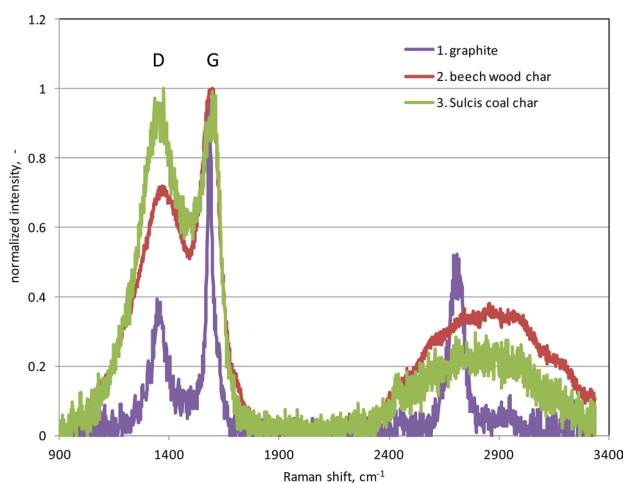
Fig. 1. Raman spectra for graphite, beech wood char, and Sulcis coal char with indication of G (1575 cm^{-1}) and D (1360 cm^{-1}) characteristic bands.

range of 500–4000 cm^{-1}. The spectra are shown in Fig. 1 for all three samples.

The test procedure for the thermoelectric measurements consists of the following steps: 1) heating the hot electrode to the desired temperature; 2) putting the sample on the two copper electrode; 3) acquiring the signals from the electrodes and the thermocouples for a certain time; and 4) removing the sample from the apparatus.

In a limited number of tests upon achieving a steady value of the temperature difference between the electrodes, a flame from a pre-mixed butane micro-burner (200 W) was applied to the center of the specimen to induce overheating. In these tests, the specimen was fixed at both ends by using screws and isolated strips. In the case of graphite, the rod was shaped to produce a thin lamina for reducing the heat transport from the specimen to the copper electrodes. These alternative tests lasted until the collapse of the specimen due to local burn-off.

The experimental results are reported and discussed in the following. Fig. 2a displays a plot of the measurements obtained at increasing temperature difference with unconverted graphite, Sulcis coal char, and beech wood char. The EMF values are well fitted by a linear interpolation versus ΔT in the first two cases, whilst a deviation from linearity is appreciable for beech wood. The graphite exhibits a positive thermoelectric effect (EMF >0), whilst both chars give negative values (EMF <0). However, this is a consequence of the adopted reference metal, copper in this case. The measured values were worked out into a thermoelectric coefficient α, calculated as the ratio between the measured ΔV and ΔT and normalized to 100 K (eq 1). It differs from the standard Seebeck coefficient because of the different reference metal (Cu instead of Pt) and sign.

$$\alpha = \Delta V / \Delta T \times 100 \qquad \mu V/100\ K \qquad (1)$$

The absolute Seebeck coefficient $\hat{\alpha}$ was calculated from α, as stated in eq 2, where 750 μV/100K is the Seebeck coefficient of the pair Cu/Pt and 510 μV/100K is the absolute Seebecck coefficient of Pt [14].
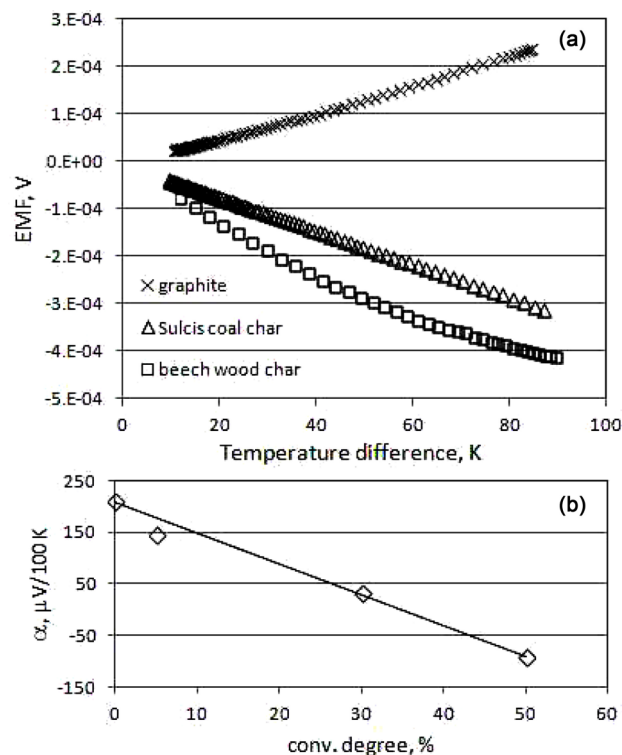

Fig. 2. Electromotive force (EMF) versus temperature difference at electrodes for graphite, Sulcis coal char, and beech wood char (a); Seebeck coefficient for graphite samples at increasing conversion degree (b).
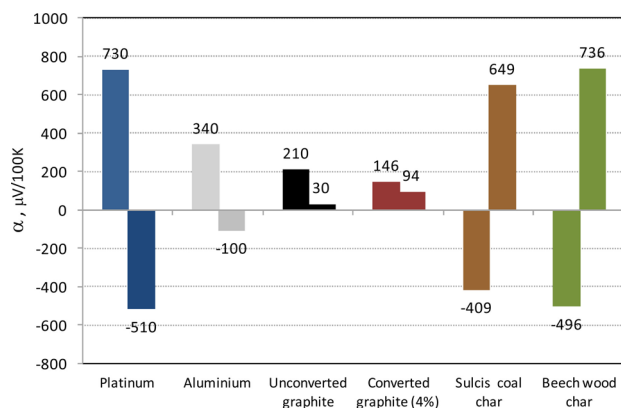
Fig. 3. Seebeck coefficient (1st bar) and absolute Seebeck coefficient (2nd bar) for different samples at ΔT of around 80°C.

$$\hat{\alpha} = 750 - \alpha - 510 \qquad \mu V/100\ K \qquad (2)$$

A comparison of the measurements for different specimens is proposed in Fig. 3, in terms of both α and $\hat{\alpha}$. The first bar represents the value obtained for the Pt lamina (730 μV/100 K), used as standard. It appears that the experimental error of the adopted technique is less than 3%, since the expected value of α would be 750 μV/100 K. The error can be attributed to presence of impurities in the copper electrodes and wires and inaccuracies of the temperature readings as well as to attenua-
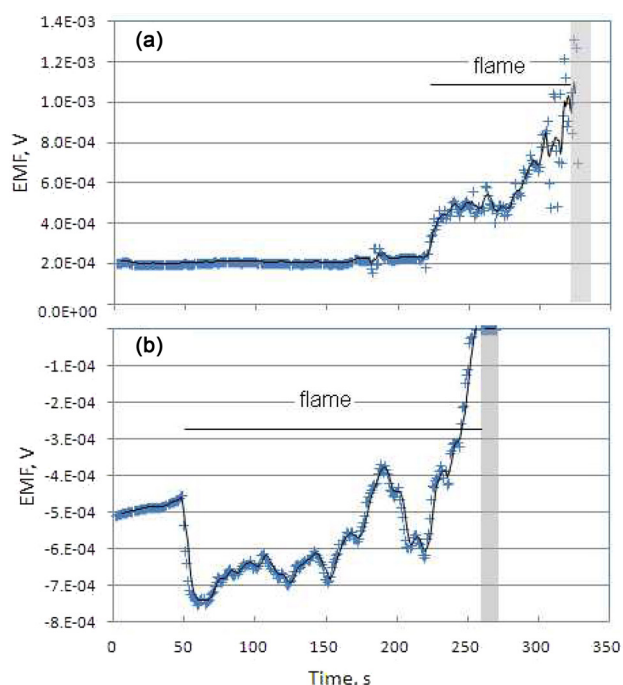
Fig. 4. Time profiles of the electromotive force for a graphite lamina (a) and a rod of beech wood char (b) in the presence of flame until collapse (gray band).

tions/noise in the electrical junctions. A measurement was also made with another metal (aluminium), giving a value of $\alpha = 340$ μV/100 K. Again, good reproducibility of the expected value was obtained, the Seebeck coefficient of the Al/Pt pair being equal to 0.39 mV/100 K [14], while the measured and normalized value is equal to 0.41 mV/100 K with a difference of only 0.02 mV/100 K.

The graphite samples, either unconverted or partly converted ($\xi = 4\%$), exhibit a positive α coefficient, whilst α is negative for beech wood and Sulcis coal chars. Regarding the absolute Seebeck coefficients, Pt and Al have negative values, whilst the carbons positive values. This means that the electric conduction mechanism changes moving from the tested metals to the carbons, with prevalence of free electrons in the former and holes in the latter [22]. Both chars exhibit a one order of magnitude higher $\hat{\alpha}$ with respect to graphite. The absolute Seebeck coefficient is higher for beech wood char than for Sulcis char, in spite of the larger ash content of the latter (Table 1). The potassium content of beech wood could be a possible explanation of this result as it would lead to a doping effect. Another possible explanation is the largely different molecular structure. In the case of beech wood, thermally degraded lignin is the main constituent of the char, giving rise to an anisotropic and oriented structure, in contrast with coal char [23]. Furthermore, the larger porosity and the lower median pore size of the beech wood char (Table 1) indicate that the continuity of the char internal structure may be more frequently interrupted. Thus, cracks and microstructural discontinuity lead to an enhanced Seebeck coefficient. The structure defects as well as the grain boundaries reduce the lattice thermal conductivity substantially via phonon scattering with a positive effect on the thermoelectric figure.

The Raman spectrum of the graphite sample (Fig. 1) reproduces typical signals of a high graphitic material with a narrow and marked G band at 1575 cm^{-1} and a less pronounced D band at 1360 cm^{-1} [24]. Conversely, the spectra of beech wood and Sulcis coal chars are characterized by a wide and pronounced D band that is an indication of the presence of defects and/or amorphous carbon [21,24]. The qualitative analysis of the Raman spectra suggests the presence of a more ordered molecular structure in the beech wood char than in the Sulcis coal char. Therefore, the trend observed for the Seebeck effect, i.e., beech wood char > Sulcis coal char > graphite (Fig. 3), does not reflect that of the structural disorder, i.e., Sulcis coal char > beech wood char > graphite. It is likely that the qualitative/quantitative difference in the content of the other elements present in the chars exerts a dominant role. Another useful information derives from correlating the measured coefficient with the sample reactivity (TG data): a marked increase of $\hat{\alpha}$ occurs moving from the less reactive (graphite) to the most porous and reactive (beech wood char) sample.

Fig. 2b displays a comparison of the measured coefficients for graphite samples at different degrees of conversion, from 0 up to 50%. The higher the conversion degree, the lower the measured coefficient is. This trend of a decreasing α with ξ could be attributed to a less connected carbon structure with a consequent decrease of the electrical conductivity as well as to the progressive enrichment in ash (Fe oxide), which could enhance the p-type behaviour of the material [25].

Tests with external heating of the specimen by means of the butane micro-burner were carried out in order to investigate the possible influence exerted by chemical reactions and overheating on the generated EMF. Fig. 4a and b show the time profiles obtained with samples of graphite and beech wood char, respectively. In both cases, when the sample was heated by the flame, a sudden and large variation of the EMF occurred towards increased absolute values of the EMF.

The change was pronounced for graphite (Fig. 4a), which exhibited an increase from 210 to 450 μV during the first 150 s after the burner ignition (t = 220 s) when the sample became red in colour at the center. The temperature of the copper electrodes remained unchanged during burner application, thanks to the high thermal inertia. The collapse of the sample was achieved at 325 s, as consequence of the chemical conversion and demolition of the connective structure. In the time immediately before the sample collapse, a steady increase of the measured EMF occurred, achieving values up to 1380 μV, likely because of the establishment of very high temperature spots in the sample.

For beech wood char, a similar response was observed, as shown in Fig. 4b. An increase of the absolute value of EMF, which rises from 500 mV to around 700 mV, occurred immediately after the flame ignition at time 50 s. The loss of the connectiveness at increasing conversion (t = 200 s) was revealed by the change of the EMF, which sharply approached zero when the sample collapsed (t = 260 s). The marked and sudden change in the measured EMF for both samples in the presence of flame can be explained by the extreme conditions, i.e., high temperature gradient, which induced drastic changes of the physical properties of the material in a delimited region of the sample.

In conclusion, an experimental technique based on thermoelectric measurements was developed for characterizing carbo-

naceous materials of different origins, as well as in the course of chemical conversion. The results of the tests performed with graphite and two different chars were very different and are related to the presence of ashes in the specimen, as well as to the fuel reactivity. The method was successfully tested for characterizing unconverted and partly converted graphite samples, proving that a connection exists between the thermoelectric response and the chemical conversion degree.

Tests made in the presence of a flame and contemporary chemical conversion of the sample proved that a sudden change of the EMF occurs, the explanation being the onset of a central region at high temperature with modified physical properties.

The absolute Seebeck coefficient of beech wood char is interestingly high, opening possibilities for application in self-sustained micro-generation, provided that char rods are properly assembled in a stack and ignited. Possible applications for chemical sensors also can be envisaged.

Conflict of Interest

No potential conflict of interest relevant to this article was reported.

References

[1] Senneca O. Kinetics of pyrolysis, combustion and gasification of three biomass fuels. Fuel Process Technol, **88**, 87 (2007). http://dx.doi.org/10.1016/j.fuproc.2006.09.002.

[2] McKee DW. Gasification of graphite in carbon dioxide and water vapor: the catalytic effects of alkali metal salts. Carbon, **20**, 59 (1982). http://dx.doi.org/10.1016/0008-6223(82)90075-6.

[3] Hurt RH, Davis KA. Near-extinction and final burnout in coal combustion. Symp (Int) Combust, **25**, 561 (1994). http://dx.doi.org/10.1016/s0082-0784(06)80686-7.

[4] Miccio F, Salatino P, Tina W. Modeling gasification and percolation of ash-bearing porous carbon particles. Proc Combust Inst, **28**, 2163 (2000). http://dx.doi.org/10.1016/s0082-0784(00)80625-6.

[5] Hoffman J, Naude G, de Beer F. 7th World Congress on Industrial Process Tomography, Kracow 780 (2013).

[6] Condon EU, Odishaw H. Handbook of Physics, Mc Graw Hill, New York (1958).

[7] Tilley RJD. Principles and Apllications of Chemical Defects, Stanley Thornes Ltd, Chetenham (1998).

[8] Rowe DM. General Principles and Basic Considerations. In: Rowe DM, ed. Thermoelectrics Handbook: Macro to Nano, Taylor & Francis, Boca Raton, 1-1 (2005).

[9] Kasap SO. Principles of Electrical Engineering Materials and Devices, McGraw-Hill, New York, 237 (1997).

[10] Tritt TM. Thermoelectric phenomena, materials, and applications. Annu Rev Mater Res, **41**, 433 (2011). http://dx.doi.org/10.1146/annurev-matsci-062910-100453.

[11] Li JF, Liu WS, Zhao LD, Zhou M. High-performance nanostructured thermoelectric materials. NPG Asia Mater, **2**, 152 (2010). http://dx.doi.org/10.1038/asiamat.2010.138.

[12] Gaultois MW, Sparks TD, Borg CKH, Seshadri R, Bonificio WD, Clarke DR. Data-driven review of thermoelectric materials: performance and resource considerations. Chem Mater, **25**, 2911 (2013). http://dx.doi.org/10.1021/cm400893e.

[13] Xie W, Weidenkaff A, Tang X, Zhang Q, Poon J, Tritt TM. Recent advances in nanostructured thermoelectric half-Heusler compounds. Nanomaterials, **2**, 379 (2012). http://dx.doi.org/10.3390/nano2040379.

[14] Cardarelli F. Materials Handbook, Springer Verlag, London (2008).

[15] Reed RP. Thermal Effects in Industrial Electronic Circuits. In: Irwin JD, ed. The Industrial Electronics Handbook, CRC Pres LLC, Boca Raton, 151 (1997).

[16] Acosta B, Sevini F. Evaluation of irradiation damage effect by applying electric properties based techniques. Nucl Eng Des, **229**, 165 (2004). http://dx.doi.org/10.1016/j.nucengdes.2003.12.009.

[17] Luo XC, Chugh R, Biller BC, Hoi YM, Chung DDL. Electronic applications of flexible graphite. J Electron Mater, **31**, 535 (2002). http://dx.doi.org/10.1007/s11664-002-0111-x.

[18] Martin J, Tritt T, Uher C. High temperature Seebeck coefficient metrology. J Appl Phys, **108**, 121101 (2010). http://dx.doi.org/10.1063/1.3503505.

[19] Park SM, Han SM, Oh SM. Characterization of artificial graphite electrodes. Carbon Lett, **1**, 76 (2000).

[20] Miccio F, Löffler G, Wargadalam VJ, Winter F. The influence of SO_2 level and operating conditions on NO_x and N_2O emissions during fluidised bed combustion of coals. Fuel, **80**, 1555 (2001). http://dx.doi.org/10.1016/s0016-2361(01)00029-1.

[21] Minutolo P, Commodo M, Santamaria A, De Falco G, D'Anna A. Characterization of flame-generated 2-D carbon nanodisks. Carbon, **68**, 138 (2014). http://dx.doi.org/10.1016/j.carbon.2013.10.073.

[22] Fujita S, Suzuki A. Electromotive Force and Measurement in Several Systems, InTech, 3 (2011).

[23] Pattanotai T, Watanabe H, Okazaki K. Gasification characteristic of large wood chars with anisotropic structure. Fuel, **117**, 331 (2014). http://dx.doi.org/10.1016/j.fuel.2013.09.030.

[24] Cuesta A, Dhamelincourt P, Laureyns J, Martínez-Alonso A, Tascón JMD. Raman microprobe studies on carbon materials. Carbon, **32**, 1523 (1994). http://dx.doi.org/10.1016/0008-6223(94)90148-1.

[25] Bagheri-Mohagheghi MM, Shahtahmasebi N, Alinejad MR, Youssefi A, Shokooh-Saremi M. Fe-doped SnO_2 transparent semiconducting thin films deposited by spray pyrolysis technique: thermoelectric and p-type conductivity properties. Solid State Sci, **11**, 233 (2009). http://dx.doi.org/10.1016/j.solidstatesciences.2008.05.005.